RESEARCH ARTICLE

Check for updates

Mechanism of formation of chiral allyl SCF₃ compounds *via* selenium-catalyzed sulfenofunctionalization of allylboronic acids†

Wen-Jie Wei, [iD] Kalman J. Szabo [iD] * and Fahmi Himo [iD] *

The detailed reaction mechanism of diphenyl selenide-catalyzed sulfenofunctionalization of chiral α-CF₃ allylboronic acids is investigated by means of density functional theory calculations. It is demonstrated that the reaction starts with the transfer of the SCF₃ group from the (PhSO₂)₂NSCF₃ reagent to the Ph₂Se catalyst, a process that is shown to be assisted by the presence of Tf₂NH acid. After a proton transfer step, the SCF₃ group is transferred to the C=C double bond of the substrate to generate a thiiranium ion. Concerted deborylative opening of the thiiranium ion yields then the final product. Several representative substrates are considered by the calculations, and the origins of the stereoselectivity of the reactions are analyzed by comparing the energies and geometries of the transition states leading to the different products.

1. Introduction

Fluorine-containing pharmacophores are often applied in modern drug substances.[1] One of five commercial drugs contains at least one C–F bond.[2] The main reason for the widespread application of fluorine-containing groups in bioactive small molecules is their beneficial metabolic and pharmacokinetical properties.[3] A particularly important pharmacophore is the trifluoromethylthio (SCF₃) group, which substantially increases the lipophilicity of the drug substances and also has a pronounced electron-withdrawing character.[4–6] As a consequence, several excellent methods appeared for the introduction of the trifluoromethylthio group to organic small molecules.[7–21] In particular, the synthesis of chirally enriched SCF₃ compounds became an important but challenging area in modern organic chemistry.[22–35]

Very recently, Szabó and co-workers presented an efficient method to introduce the SCF₃ group by using (PhSO₂)₂NSCF₃ reagent[36] **2** with α-CF₃ allylboronic acid derivatives **1** to form a chiral alkenyl SCF₃ compound **5** (Scheme 1).[37] The reaction relies on the application of selenium-based Lewis base Ph₂Se **3** as a catalyst in the presence of Tf₂NH **4** as the activator. These reactions have a high degree of functional group tolerance and proceed with excellent stereo-, diastereo- and site-selectivity.

The application of electrophilic sulfenofunctionalization in the presence of selenium catalysis has been documented by the pioneering studies of the groups of Denmark,[38] Zhao,[26] and others.[39] However, the application of allylboronate substrates for trifluoromethylthiolation revealed a couple of new, interesting mechanistic aspects.[37] An important feature is the excellent stereochemistry of the reaction, including chirality transfer and high *E*-selectivity for the formation of the new double bond. The studies also pointed out the benefits of using allylboronic acid type of substrates. Replacement of the B(OH)₂ group of **1** with Bpin leads to a significant decrease in the yield of the product, indicating that allyl-Bpin species have a substantially lower reactivity than allylboronic acids.

In the present work, we have performed density functional theory (DFT) calculations to elucidate the mechanism for the formation of allyl SCF₃ compounds *via* the selenium-catalyzed sulfenofunctionalization of allylboronic acids. We consider the reactions of several representative substrates (**1a–1d** in Scheme 1) and discuss the origins of selectivity for each of them.
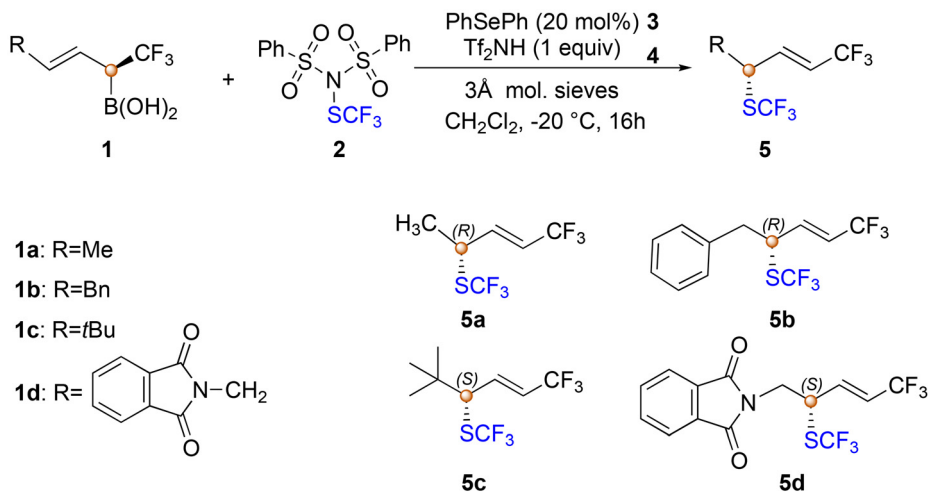
2. Computational details

The B3LYP-D3(BJ) functional,[40,41] which includes the D3 dispersion correction with the Becke–Johnson damping function,[42,43] was used for all calculations presented in this work, and the Gaussian 16 program[44] was employed. Geometry optimizations were carried out with the 6-31G(d,p) basis set. To obtain more accurate energies, single-point calculations were performed on the optimized structures using the larger basis set 6-311+G(2d,2p). Analytical frequency calculations were performed at the level of theory of the geometry optimization to calculate the Gibbs free energy corrections. Solvation

Department of Chemistry, Arrhenius Laboratory, Stockholm University, SE-106 91 Stockholm, Sweden. E-mail: kalman.j.szabo@su.se, fahmi.himo@su.se

2994 | *Org. Chem. Front.*, 2025, **12**, 2994–3003

This journal is © the Partner Organisations 2025

Scheme 1 Se-catalyzed sulfenofunctionalization of allylboronic acid to form chiral allyl SCF₃ compound investigated in the present study.

effects were considered by performing single-point calculations on the optimized structures using the SMD method[45] with the parameters of dichloromethane.
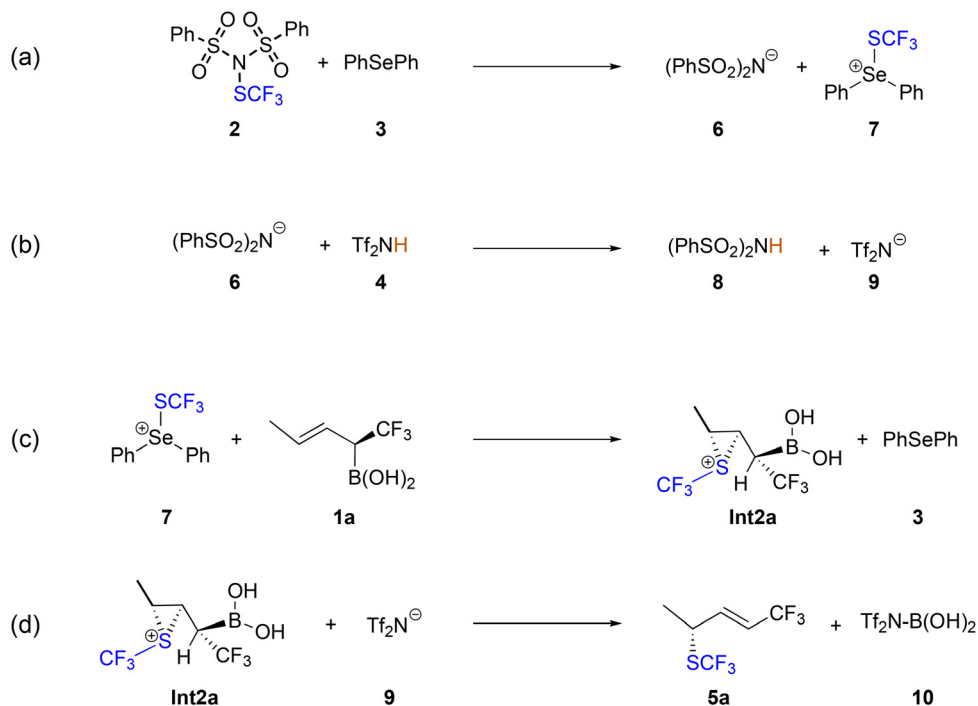
To evaluate the effect of performing the geometry optimizations with the smaller basis set and in the gas phase, the geometries of the first step of the reaction (**2** + **3** + **4** → **Int1**, see below) were re-optimized twice, in implicit DCM solvent and with the larger basis set. The calculations showed that the geometries and energies were not affected significantly (see ESI†).

Intrinsic reaction coordinate (IRC) calculations were performed on all transition states to confirm the nature of the

connecting intermediates. A thorough manual conformation search was carried out on all stationary points to ensure that the structures with the lowest energy were located.

3. Results and discussion

We start the mechanistic investigation by considering the reaction of model substrate **1a**, in which the R group is a simple methyl substituent. Although this compound was not included in the experimental studies,[37] it can serve as a good reference

Scheme 2 Reaction steps investigated in the present study.

This journal is © the Partner Organisations 2025

Org. Chem. Front., 2025, **12**, 2994–3003 | **2995**

for γ-alkyl allylboronates. As representatives for different classes of substrates, we subsequently investigate the mechanisms of three other substrates that have been examined explicitly by the experiments,[37] namely those in which the R is a relatively bulky benzyl (**1b**) and *tert*-butyl (**1c**) groups, as well as a nitrogen-containing phthalimide derivative **1d** (Scheme 1).

3.1. Reaction of model substrate 1a

The first step of the reaction mechanism is the transfer of the SCF$_3$ group from the (PhSO$_2$)$_2$NSCF$_3$ transfer reagent **2** to the Ph$_2$Se catalyst **3**, generating the SePh$_2$SCF$_3$ cation **7** (Scheme 2a). We found that this step is assisted by the participation of Tf$_2$NH acid **4** that forms a hydrogen bond to the

nitrogen of the transfer reagent (**TS1**, Fig. 1). The calculated barrier is 24.2 kcal mol^{-1}, and the energy of the resulting intermediate **Int1**, in which acid **4**, the (PhSO$_2$)$_2$N$^-$ anion **6** and the SePh$_2$SCF$_3$ cation **7** are in complex with each other, lies at 21.3 kcal mol^{-1} (Fig. 2). The hydrogen bond provided by acid **4** stabilizes the negative charge developing on the nitrogen atom, as seen from the H···N distance, which is 1.98 Å at **TS1** and 1.86 Å at **Int1**. Transfer of the SCF$_3$ group without the participation of the acid was also considered and was found to have a much higher energy barrier of 50.4 kcal mol^{-1} (see ESI†).

Next step is a proton transfer from **4** to (PhSO$_2$)$_2$N$^-$ anion **6** *via* **TS2**, generating (PhSO$_2$)$_2$NH **8** and Tf$_2$N$^-$ anion **9**
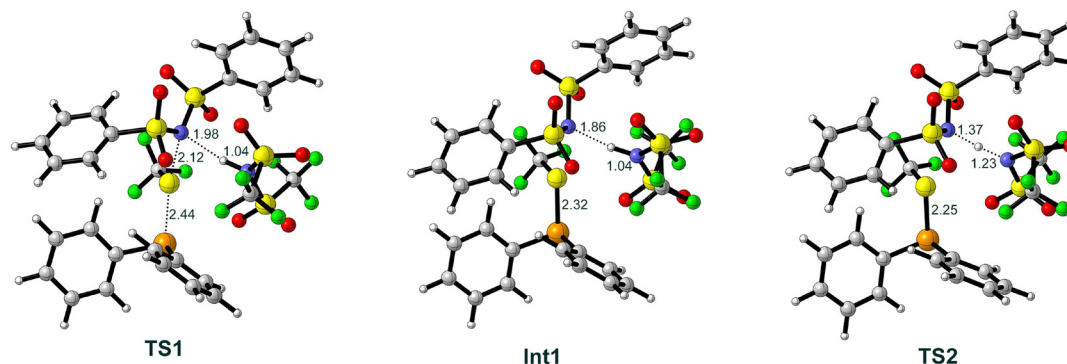

Fig. 1 Optimized structures of the transition states and intermediates of **TS1**, **Int1**, and **TS2**. Selected bond distances are indicated in Å.
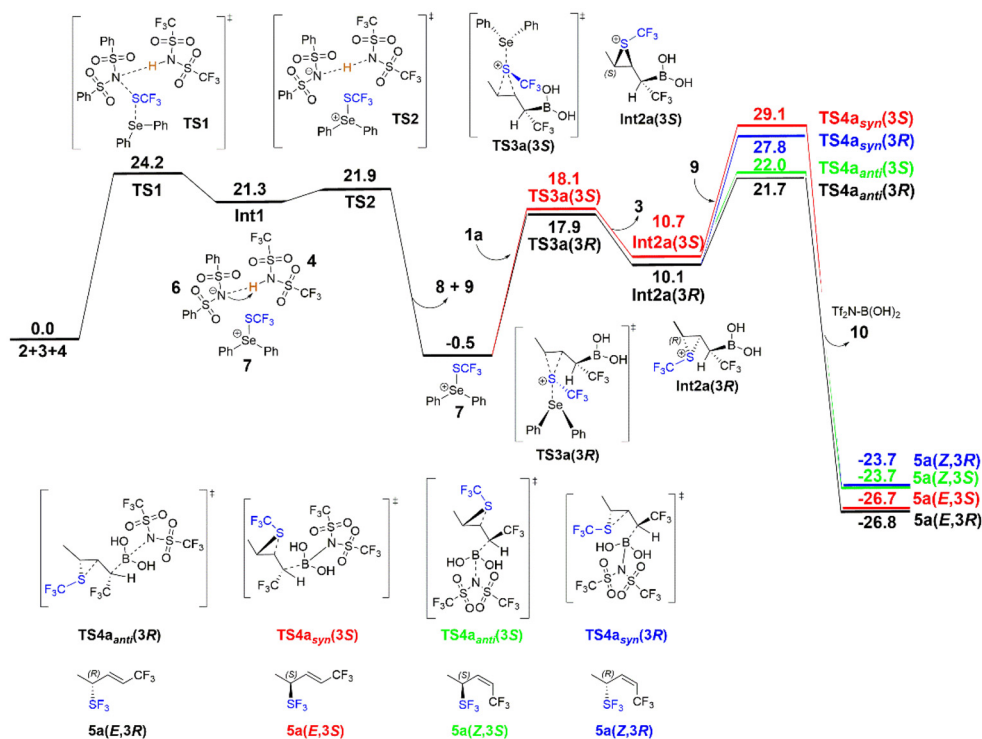

Fig. 2 Calculated free energy profile (kcal mol^{-1}) of model substrate **1a**.

2996 | *Org. Chem. Front.*, 2025, **12**, 2994–3003

This journal is © the Partner Organisations 2025
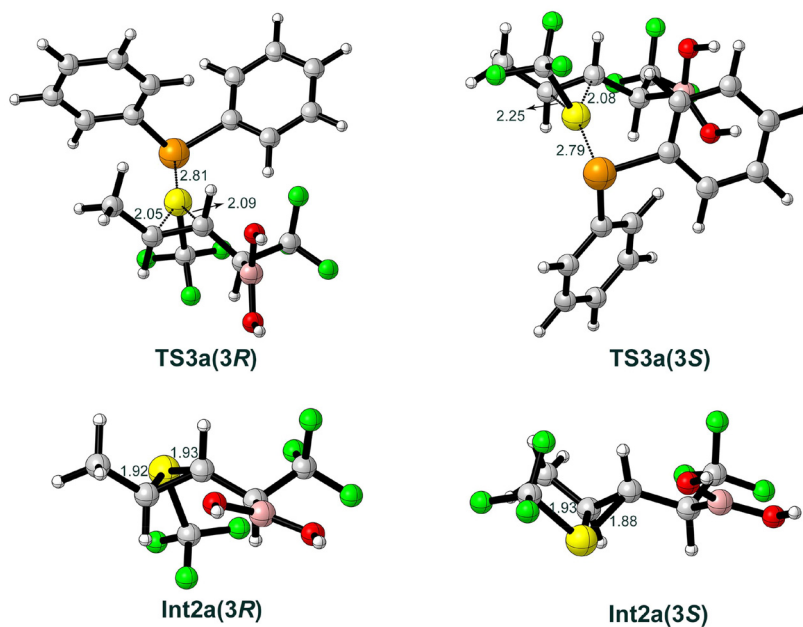
Fig. 3 Optimized structures of the transition states and intermediates for the generation of the thiiranium ion **Int2a**. Selected bond distances are indicated in Å.
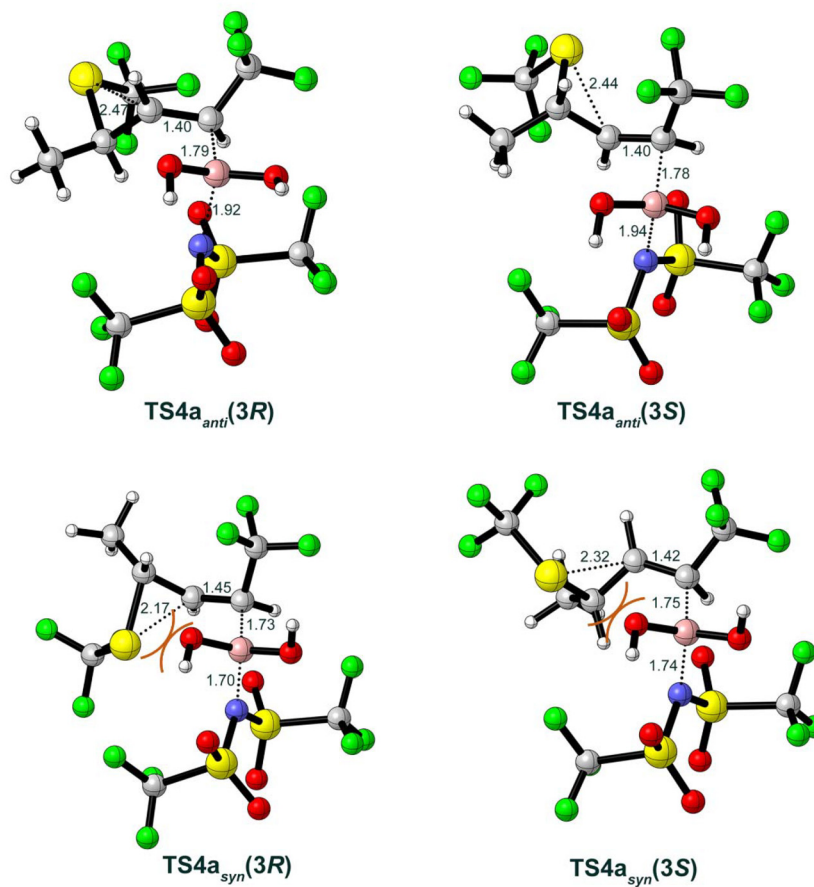

Fig. 4 Optimized structures of the transition states for the step of deborylative elimination in model substrate **1a**. Selected bond distances are indicated in Å.

This journal is © the Partner Organisations 2025

Org. Chem. Front., 2025, **12**, 2994–3003 | **2997**

(Scheme 2b). The energy barrier of this step is only 0.6 kcal mol^{-1} relative to **Int1**.

We also calculated the alternative pathway with the reversed step order, *i.e.* in which a proton is first transferred from acid **4** to (PhSO$_2$)$_2$NSCF$_3$, followed by the transfer of the SCF$_3$ group from the generated (PhSO$_2$)$_2$NHSCF$_3$ cation to the Ph$_2$Se catalyst **3**. However, the energy barrier of this scenario was found to be very high, 52.9 kcal mol^{-1} (see ESI†).

In the following step of the mechanism, the SCF$_3$ group of the SePh$_2$SCF$_3$ cation **7** is transferred to the C=C double bond of the substrate to generate a thiiranium ion (Scheme 2c). Two competing stereoselective pathways are possible and were investigated, in which the SCF$_3$ group is transferred either to the *Re*-face of the substrate *via* **TS3a(3R)** to form the (*R*)-configuration **Int2a(3R)**, or to the *Si*-face *via* **TS3a(3S)** to generate the (*S*)-configuration **Int2a(3S)**. The optimized structures of the transition states and intermediates are shown in Fig. 3. The energies of **TS3a(3R)** and **TS3a(3S)** are calculated to be 18.4 and 18.6 kcal mol^{-1}, respectively, relative to the previous intermediate, and the resulting **Int2a(3R)** and **Int2a(3S)** are 10.6 and 11.2 kcal mol^{-1} higher, respectively.

For comparison, we also investigated the uncatalyzed reaction, in which the SCF$_3$ group is transferred directly from reagent **2** to substrate **1a**, generating **Int2a** without the participation of catalyst **3** (see ESI†). The energy barrier was calculated to be 29.9 kcal mol^{-1} for both the 3*R*- and 3*S*-pathways, which is significantly higher than the case with catalyst **3**. Accordingly, using PhSePh catalyst (**3**) increases the reactivity of **2**. In the positively charged **7** the electrophilicity of SCF$_3$ is substantially increased compared to **2**. In addition, the cleavage of the weak Se–S bond in **7** is also easier than the cleavage of the N–S bond of **2**. The stability of **7** is poor under ambient conditions, and therefore **2** is converted to **7** *in situ* (in the presence of **4**) under the applied reaction conditions.

The final step of the mechanism (Scheme 2d) involves the Tf$_2$N$^-$ anion **9** performing a nucleophilic attack on the boronate group of **Int2a(3R)** or **Int2a(3S)**, triggering the concerted deborylative opening of the thiiranium ion *via* **TS4** to yield the four possible forms of the final product. The (3*R*)-configured products are formed from **Int2a(3R)** and can result in either the *E*-configuration through the *anti*-elimination pathway *via* **TS4$_{anti}$(3R)**, or alternatively, rotation of the C$_\alpha$–C$_\beta$ bond leads to the *syn*-elimination pathway *via* **TS4$_{syn}$(3R)**, resulting in the *Z*-configuration. Similarly, the *E*-(3*S*)- or *Z*-(3*S*)-configured products can be achieved *via* **TS4$_{syn}$(3S)** or **TS4$_{anti}$(3S)**, respectively. The optimized structures of these transition states are shown in Fig. 4, while the optimized structures of the products are given in the ESI.†
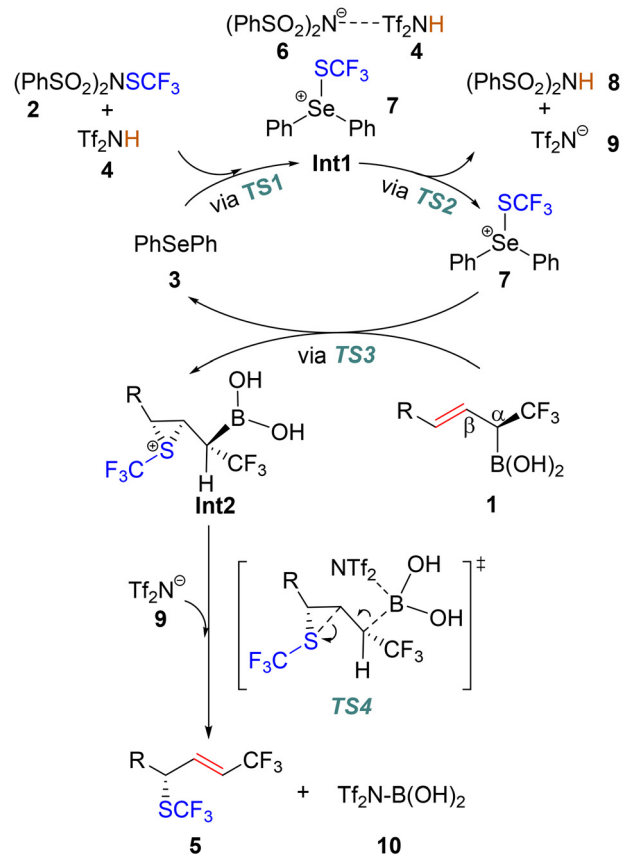
Although the chiral center is formed at **TS3**, the calculations show that the energy barriers for the eliminations of the boronate group *via* **TS4** are higher and irreversible, which means that the latter step is the stereoselectivity-determining step of the reaction.

By comparing the energy profiles of the above four pathways (Fig. 2), the calculations of the model substrate **1a** show that the energy barriers of *anti*-eliminations are considerably

lower than the *syn*-eliminations, 21.7 kcal mol^{-1} in **TS4$_{anti}$(3R)** *vs.* 27.8 kcal mol^{-1} in **TS4$_{syn}$(3R)**, and 22.0 kcal mol^{-1} in **TS4$_{anti}$(3S)** *vs.* 29.1 kcal mol^{-1} in **TS4$_{syn}$(3S)**. Inspection of the optimized structures in Fig. 4 shows that the reason for this energy difference is mainly the steric repulsion between the SCF$_3$ group and the leaving boronate group, as these two moieties point toward each other in the *syn*-elimination, **TS4$_{syn}$(3R)** and **TS4$_{syn}$(3S)**, while in the *anti*-elimination, **TS4$_{anti}$(3R)** and **TS4$_{anti}$(3S)**, they point away from each other.

The difference in energy between **TS4$_{anti}$(3R)** and **TS4$_{anti}$(3S)**, which lead to the *E*-(3*R*)-5a and *Z*-(3*S*)-5a products, respectively, is calculated to be only 0.3 kcal mol^{-1} in favor of the former. The calculations show thus that already the model substrate **1a**, with the small methyl substituent, qualitatively reproduces the experimental selectivity trend, in that the formation of the *E*-(3*R*)-configured product is associated with the lowest-energy pathway, albeit with a small energy. However, as will be shown below, the calculations using the experimentally employed substrates, with bulkier substituents, yield a more quantitative agreement with the experiments.

To summarize, the mechanism proposed on the basis of the current calculations is given in Scheme 3. The obtained overall energy profile (Fig. 2) indicates that the first step, *i.e.* the acid-assisted transfer of the SCF$_3$ group *via* **TS1**, is the rate-

Scheme 3 Reaction mechanism suggested on the basis of the current calculations.

2998 | *Org. Chem. Front.*, 2025, **12**, 2994–3003

This journal is © the Partner Organisations 2025

determining step (RDS) for the model substrate, with a barrier of 24.2 kcal mol⁻¹. However, the final step, *i.e.* deborylative opening of the thiiranium ring *via* **TS4**, has an overall barrier of 22.2 kcal mol⁻¹, which is quite close in energy, and it is therefore not possible to determine confidently the nature of the RDS based only on the calculations. In particular, various substituents on the substrate may lead to significant changes in the energy of the final step (see below).

Here, it is interesting to mention two previous mechanistic studies on sulfenofunctionalizations of alkenes catalyzed by selenides, where DFT calculations were employed to investigate various aspects of the reactions. However, none of these studies involved a deborylation step, which is a novel aspect of the present study. Denmark and co-workers analyzed the geometries and energies of the transition states for the thiiranium ion formation step, which was assumed to be the enantio-determining step of the reaction,[46] while Zhao and co-workers investigated the mechanism of selenide-catalyzed trifluoromethylthiolation of *gem*-diaryl tethered alkenes to synthesize trifluoromethylthiolated tetrahydronaphthalenes.[27]

In addition to the results discussed above, we have also considered some other mechanistic alternatives that turned out to have higher energy barriers. As seen from Fig. 2 and 4, catalyst **3** does not participate in the deborylative elimination step in **TS4**. We have considered whether it can assist this step, but the energy barriers for this scenario were found to be higher (see ESI†). We also considered whether the $(PhSO_2)_2NH$ species **8** could act as the nucleophile to attack the boronate group of **Int2a**, but the calculated energy barriers for this pathway were calculated to be very high as compared to when the anionic Tf_2N^- **9** is the nucleophile (see ESI†). Finally, the experiments reveal that replacing the $B(OH)_2$ group of the substrate with Bpin significantly decreases the yield of the product.[37] Consistently with this result, the calculations show that the barrier for the case of Bpin is 3.7 kcal mol⁻¹ higher than the case of the $B(OH)_2$ group (see ESI†).

3.2. Reactions with other substrates

Next, we calculated the mechanisms when the R group of the substrate is Bn (**1b**), *t*Bu (**1c**), and the phthalimide substituent
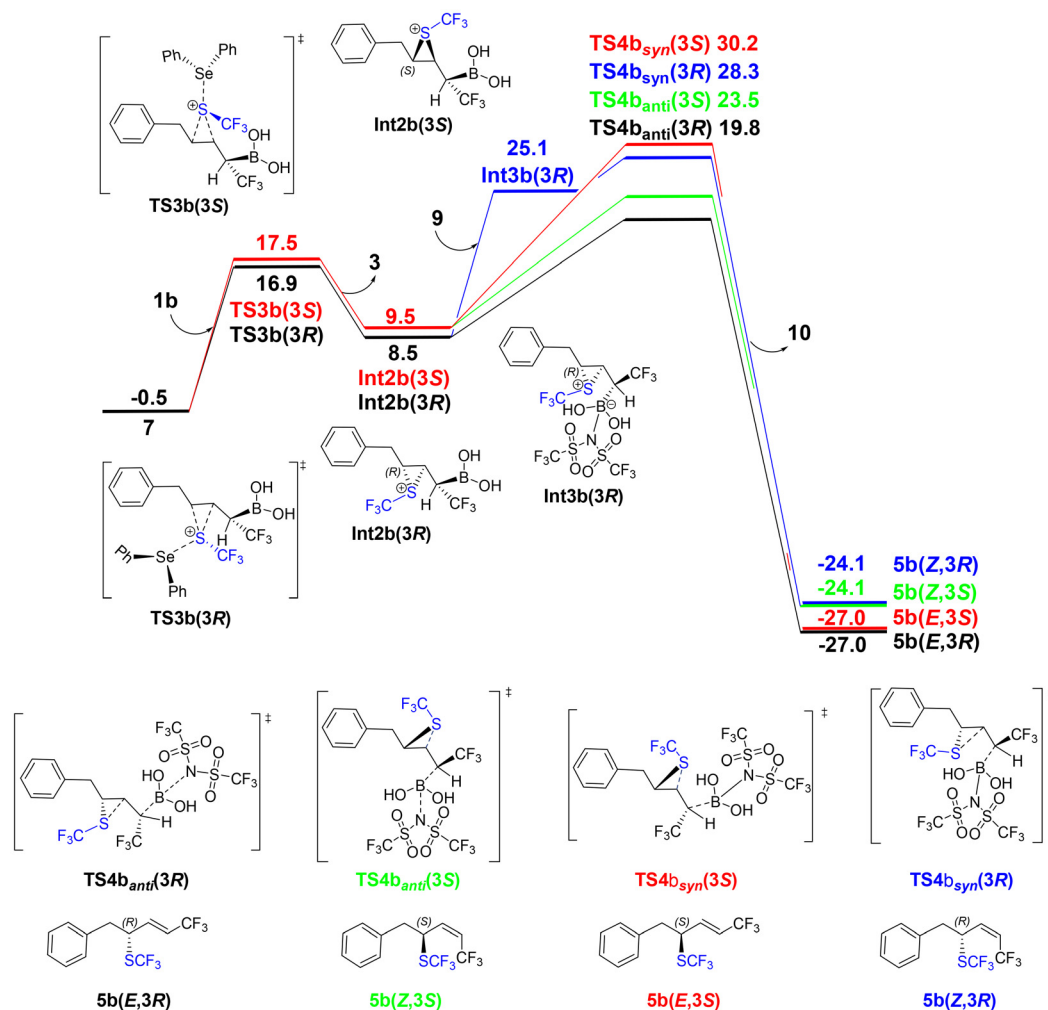

Fig. 5 Calculated free energy profile (kcal mol⁻¹) of substrate **1b**.

This journal is © the Partner Organisations 2025

Org. Chem. Front., 2025, **12**, 2994–3003 | **2999**

(**1d**), all of which have been employed in the experimental study.[37] As seen from Fig. 2, the reaction mechanism up to the formation of SePh$_2$SCF$_3$ cation **7** is independent of the substrate, and therefore we investigated the reactions of the other substrates starting from this point.

For substrate **1b**, with the benzyl substituent, the mechanism was calculated to be very similar to that of the model substrate **1a** shown in Scheme 3 (see calculated energy profile in Fig. 5). One small difference is that the formation of the *Z*-(3*R*)-configured product through the *syn*-elimination was found to occur in a stepwise manner (see ESI† for detailed results). The calculations show that the overall barrier for substrate **1b** is *ca.* 2 kcal mol⁻¹ lower than for **1a**, and very importantly, the extent of the stereo-differentiation is well-reproduced.

Similarly to substrate **1a**, the barriers of *anti*-eliminations for **1b** are considerably lower than the *syn*-eliminations due to steric repulsion between the SCF$_3$ group and the leaving boronate group. In addition, the pathway leading to the ***E*-(3*R*)-5b** product is now 3.7 kcal mol⁻¹ lower than that leading to the ***Z*-(3*S*)-5b** product (Fig. 5), due to a steric repulsion between the benzyl substituent of the substrate and the SCF$_3$ group (see ESI†). The calculated energy difference is in good agreement with the experimentally observed ee of 93% in favor of the *E*-(3*R*) product.

For substrate **1c** with the *t*Bu substituent (see ESI†), the situation is very similar to substrate **1b**, with both *syn*-eliminations found to take place in a stepwise manner. The overall barrier was calculated to be *ca.* 3 kcal mol⁻¹ higher than for **1b**, and the selectivity is determined by the same factors, with
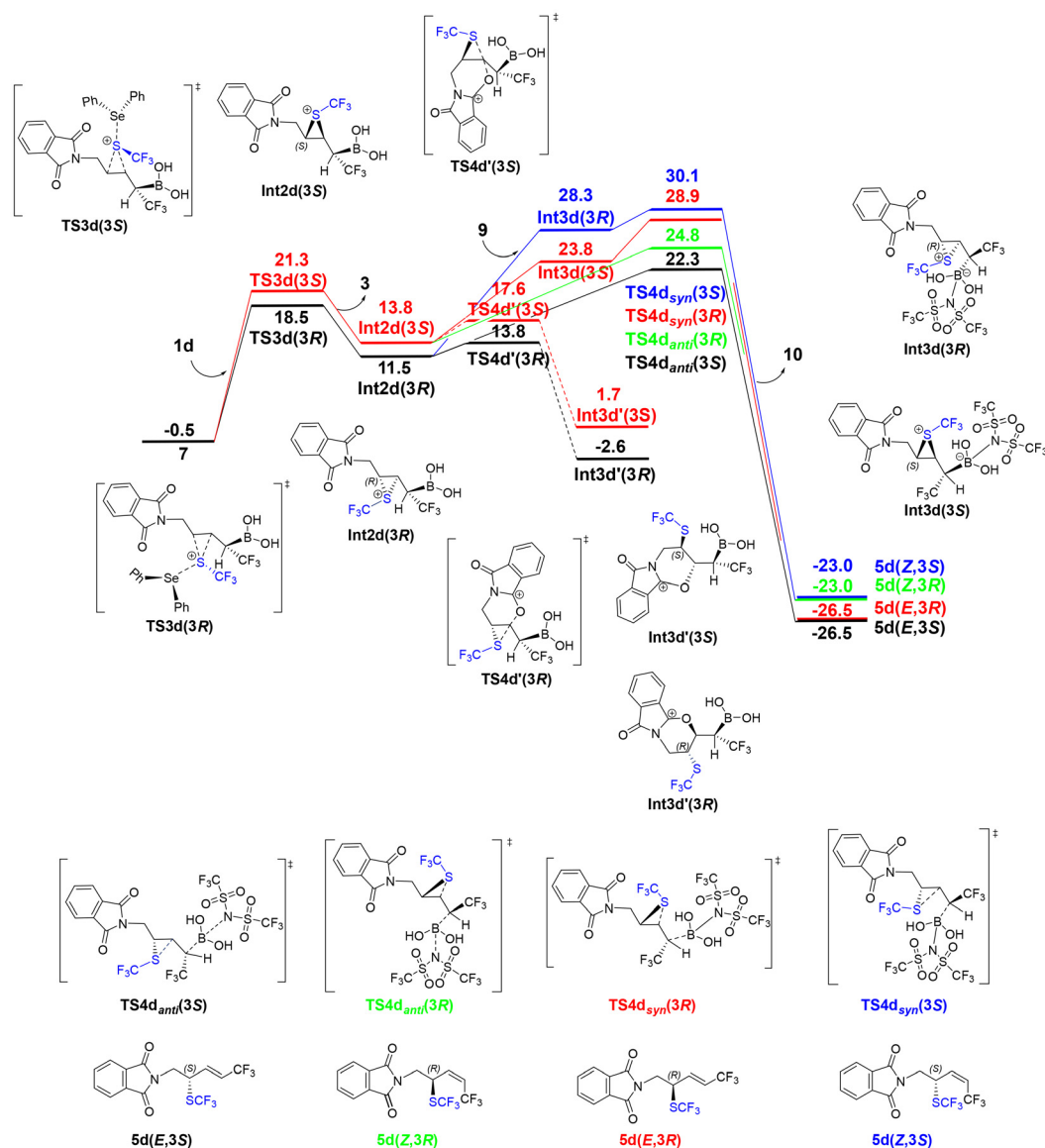

Fig. 6 Calculated free energy profile (kcal mol⁻¹) of substrate **1d**.

3000 | *Org. Chem. Front.*, 2025, **12**, 2994–3003

This journal is © the Partner Organisations 2025

an energy difference of 4.2 kcal mol^{-1}, in good agreement with the experimental outcome of 98% ee.

Substrate **1d**, with the phthalimide substituent, represents an interesting case, because the carbonyl group of **1d** may perform a nucleophilic attack at the C_β atom of the thiiranium ion through an intramolecular mechanism,[25,47,48] leading to the opening of the thiiranium ion and yielding a six-membered ring intermediate **Int3d′** (see Fig. 6). The calculations show that the energy barrier for this competing intramolecular nucleophilic attack via **TS4d′** is much lower than for the intermolecular reaction of the thiiranium ion with the Tf_2N^- anion **9** via **TS4d**, which was found for the other substrates. However, from **Int3d′**, the barriers for the following steps, which would be the nucleophilic attack of Tf_2N^- and the deborylative opening of the six-membered ring, were found to be higher in energy compared to the intermolecular reaction (see ESI†), indicating that the intramolecular nucleophilic attack is a reversible process. Thus, formation of **Int3d′** can be regarded as an unproductive dead-end for the deborylative trifluoromethylthiolation process.

The calculations show thus that the reaction of substrate **1d** also follows the mechanism of the model substrate **1a**. However, as seen from Fig. 6, the energy of **Int3d′** is the lowest point on the energy profile before **TS4d**, which means that the overall barrier should be calculated relative to **Int3d′**, resulting in a slightly higher barrier as compared to the other substrates (24.9 kcal mol^{-1} compared to 22.2, 20.3, and 23.2 kcal mol^{-1}, for **1a**, **1b** and **1c**, respectively). Importantly, the stereoselectivity is reproduced also for substrate **1d**, with a selectivity-determining energy difference of 2.5 kcal mol^{-1}, in good agreement with the 97% ee observed experimentally. The origins of the selectivity are found to be the same as for the other substrates.

4. Conclusions

In the present work, the reaction mechanism for the formation of chiral allyl SCF_3 compounds via diphenyl selenide-catalyzed sulfenofunctionalization of allylboronic acids has been investigated using DFT calculations. Several allylboronic acid substrates were considered, and the mechanism suggested on the basis of the calculations is shown in Scheme 2.

The reaction starts with the generation of the catalytically active $SePh_2SCF_3$ cation, a process that takes place is in a stepwise manner, with a transfer of the SCF_3 group from the $(PhSO_2)_2NSCF_3$ reagent **2** to the Ph_2Se catalyst **3**, followed by a proton transfer from acid Tf_2NH **4** to the formed $(PhSO_2)_2N^-$ anion **6**. Interestingly, the Tf_2NH acid stabilizes the negative charge that develops on the nitrogen anion of the $(PhSO_2)_2N^-$ species **6** through a hydrogen bond interaction, lowering thus the barrier for the SCF_3 transfer.

Next, the SCF_3 group of the formed $SePh_2SCF_3$ cation is transferred to the C=C bond of the α-CF_3 allylboronic acid, generating the thiiranium ion species **Int2**. Two different pathways are possible, depending on whether the SCF_3 group is transferred to the *Si* or *Re* face of the C=C bond, which eventually lead to the *S*- or *R*-configurations of the product, respectively.

Finally, the Tf_2N^- anion **9** performs a nucleophilic attack at the boronate group of **Int2**, triggering the opening of the thiiranium ion and the leaving of the boronate group. Rotation around the C_α–C_β bond of **Int2** leads to either the *syn*- or *anti*-elimination, generating the *E*- or *Z*- configurations of the product. This step constitutes the selectivity-determining step of the reaction, and the calculations show a clear preference for formation of the *E*-form, in excellent agreement with the high *E*-selectivity reported in the experimental studies.[37] The enantioselectivity is also very well reproduced by the calculations, and analysis of the transition state structures shows that the selectivity is mainly controlled by steric repulsions between the SCF_3 group and both the leaving boronate group and the substituent of the α-CF_3 allylboronic acid.

The mechanistic insights provided by the current study will be valuable for the development of new regio-, stereo- and diastero-selective selenide-catalyzed, deborylative electrophilic sulfenofunctionalization reactions.

Data availability

The data supporting this article have been included as part of the ESI.†

Conflicts of interest

There are no conflicts to declare.

Acknowledgements

References

1 Y. Zhu, J. Han, J. Wang, N. Shibata, M. Sodeoka, V. A. Soloshonok, J. A. S. Coelho and F. D. Toste, Modern Approaches for Asymmetric Construction of Carbon-Fluorine Quaternary Stereogenic Centers: Synthetic Challenges and Pharmaceutical Needs, *Chem. Rev.*, 2018, **118**(7), 3887–3964.

2 H. Mei, J. Han, S. Fustero, M. Medio-Simon, D. M. Sedgwick, C. Santi, R. Ruzziconi and V. A. Soloshonok, Fluorine-Containing Drugs Approved by the FDA in 2018, *Chem. – Eur. J.*, 2019, **25**(51), 11797–11819.

3 Y. Zhou, J. Wang, Z. Gu, S. Wang, W. Zhu, J. L. Aceñ, V. A. Soloshonok, K. Izawa and H. Liu, Next Generation of Fluorine-Containing Pharmaceuticals, Compounds

This journal is © the Partner Organisations 2025

Org. Chem. Front., 2025, **12**, 2994–3003 | **3001**

Currently in Phase II-III Clinical Trials of MajorPharmaceutical Companies: New Structural Trends and TherapeuticAreas, *Chem. Rev.*, 2016, **116**(2), 422–518.

4 C. Hansch, A. Leo and R. W. Taft, A survey of Hammett substituent constants and resonance and field parameters, *Chem. Rev.*, 1991, **91**(2), 165–195.

5 E. A. Ilardi, E. Vitaku and J. T. Njardarson, Data-Mining for Sulfur and Fluorine: An Evaluation of Pharmaceuticals to Reveal Opportunities for Drug Design and Discovery, *J. Med. Chem.*, 2014, **57**(7), 2832–2842.

6 D. O'Hagan, Understanding organofluorine chemistry. An introduction to the C–F bond, *Chem. Soc. Rev.*, 2008, **37**(2), 308–319.

7 Q. Shen, A Toolbox of Reagents for Trifluoromethylthiolation: From Serendipitous Findings to Rational Design, *J. Org. Chem.*, 2023, **88**(6), 3359–3371.

8 Y.-D. Yang, A. Azuma, E. Tokunaga, M. Yamasaki, M. Shiro and N. Shibata, Trifluoromethanesulfonyl Hypervalent Iodonium Ylide for Copper-Catalyzed Trifluoromethylthiolation of Enamines, Indoles, and β-Keto Esters, *J. Am. Chem. Soc.*, 2013, **135**(24), 8782–8785.

9 S. Arimori, M. Takada and N. Shibata, Trifluoromethylthiolation of Allylsilanes and Silyl Enol Ethers with Trifluoromethanesulfonyl Hypervalent Iodonium Ylide under Copper Catalysis, *Org. Lett.*, 2015, **17**(5), 1063–1065.

10 Z. Huang, Y.-D. Yang, E. Tokunaga and N. Shibata, Copper-Catalyzed Regioselective Trifluoromethylthiolation of Pyrroles by Trifluoromethanesulfonyl Hypervalent Iodonium Ylide, *Org. Lett.*, 2015, **17**(5), 1094–1097.

11 F. Baert, J. Colomb and T. Billard, Electrophilic trifluoromethanesulfanylation of organometallic species with trifluoromethanesulfanamides, *Angew. Chem., Int. Ed.*, 2012, **51**(41), 10382–10385.

12 S. Rossi, A. Puglisi, L. Raimondi and M. Benaglia, Synthesis of Alpha-trifluoromethylthio Carbonyl Compounds: A Survey of the Methods for the Direct Introduction of the SCF3 Group on to Organic Molecules, *ChemCatChem*, 2018, **10**(13), 2717–2733.

13 S. Alazet, L. Zimmer and T. Billard, Electrophilic Trifluoromethylthiolation of Carbonyl Compounds, *Chem. – Eur. J.*, 2014, **20**(28), 8589–8593.

14 W. Tyrra, D. Naumann, B. Hoge and Y. L. Yagupolskii, A New Synthesis of Trifluoromethanethiolates-Characterization and Properties of Tetramethylammonium, Cesium and Di(benzo-15-crown-5)cesium Trifluoromethanethiolates, *J. Fluor. Chem.*, 2003, **119**(1), 101–107.

15 Z. Weng, W. He, C. Chen, R. Lee, D. Tan, Z. Lai, D. Kong, Y. Yuan and K.-W. Huang, An Air-Stable Copper Reagent for Nucleophilic Trifluoromethylthiolation of Aryl Halides, *Angew. Chem., Int. Ed.*, 2013, **52**(5), 1548–1552.

16 D. Kong, Z. Jiang, S. Xin, Z. Bai, Y. Yuan and Z. Weng, Room Temperature Nucleophilic Trifluoromethylthiolation of Benzyl Bromides with (bpy)Cu(SCF₃), *Tetrahedron*, 2013, **69**(30), 6046–6050.

17 J. Tan, G. Zhang, Y. Ou, Y. Yuan and Z. Weng, Nucleophilic Trifluoromethylthiolation of Allylic Bromides: A Facile Preparation of Allylic Trifluoromethyl Thioethers, *Chin. J. Chem.*, 2013, **31**(7), 921–926.

18 Q. Lin, L. Chen, Y. Huang, M. Rong, Y. Yuan and Z. Weng, Efficient C(sp³$_{alkyl}$)-SCF₃ Bond Formations via Copper-mediated Trifluoromethylthiolation of Alkyl Halides, *Org. Biomol. Chem.*, 2014, **12**(29), 5500–5508.

19 S. Dix, M. Jakob and M. N. Hopkinson, Deoxytrifluoromethylthiolation and Selenylation of Alcohols by Using Benzothiazolium Reagents, *Chem. – Eur. J.*, 2019, **25**(32), 7635–7639.

20 X.-H. Xu, K. Matsuzaki and N. Shibata, Synthetic Methods for Compounds Having CF₃-S Units on Carbon by Trifluoromethylation, Trifluoromethylthiolation, Triflylation, and Related Reactions, *Chem. Rev.*, 2015, **115**(2), 731–764.

21 C. Ghiazza, T. Billard and A. Tlili, Merging Visible-Light Catalysis for the Direct Late-Stage Group-16−Trifluoromethyl Bond Formation, *Chem. – Eur. J.*, 2019, **25**(26), 6482–6495.

22 T. Bootwicha, X. Liu, R. Pluta, I. Atodiresei and M. Rueping, N-Trifluoromethylthiophthalimide: A Stable Electrophilic SCF₃-Reagent and its Application in the Catalytic Asymmetric Trifluoromethylsulfenylation, *Angew. Chem., Int. Ed.*, 2013, **52**(49), 12856–12859.

23 X. Wang, T. Yang, X. Cheng and Q. Shen, Enantioselective Electrophilic Trifluoromethylthiolation of β-Ketoesters: A Case of Reactivity and Selectivity Bias for Organocatalysis, *Angew. Chem., Int. Ed.*, 2013, **52**(49), 12860–12864.

24 X.-L. Zhu, J.-H. Xu, D.-J. Cheng, L.-J. Zhao, X.-Y. Liu and B. Tan, In Situ Generation of Electrophilic Trifluoromethylthio Reagents for Enantioselective Trifluoromethylthiolation of Oxindoles, *Org. Lett.*, 2014, **16**(8), 2192–2195.

25 X. Liu, R. An, X. Zhang, J. Luo and X. Zhao, Enantioselective Trifluoromethylthiolating Lactonization Catalyzed by an Indane-Based Chiral Sulfide, *Angew. Chem., Int. Ed.*, 2016, **55**(19), 5846–5850.

26 X. Liu, Y. Liang, J. Ji, J. Luo and X. Zhao, Chiral Selenide-Catalyzed Enantioselective Allylic Reaction and Intermolecular Difunctionalization of Alkenes: Efficient Construction of C-SCF₃ Stereogenic Molecules, *J. Am. Chem. Soc.*, 2018, **140**(14), 4782–4786.

27 J. Luo, Q. Cao, X. Cao and X. Zhao, Selenide-catalyzed enantioselective synthesis of trifluoromethylthiolated tetrahydronaphthalenes by merging desymmetrization and trifluoromethylthiolation, *Nat. Commun.*, 2018, **9**(1), 527.

28 T. Qin, Q. Jiang, J. Ji, J. Luo and X. Zhao, Chiral Selenide-Catalyzed Enantioselective Synthesis of Trifluoromethylthiolated 2,5-Disubstituted Oxazolines, *Org. Biomol. Chem.*, 2019, **17**(7), 1763–1766.

29 M. Y. Jin, J. Li, R. Huang, Y. Zhou, L. W. Chung and J. Wang, Catalytic Asymmetric Trifluoromethylthiolation of Carbonyl Compounds via a Diastereo and Enantioselective Cu-Catalyzed Tandem Reaction, *Chem. Commun.*, 2018, **54**(36), 4581–4584.

3002 | *Org. Chem. Front.*, 2025, **12**, 2994–3003

This journal is © the Partner Organisations 2025

30 L. Xu, L. Yu, J. Liu, H. Wang, C. Zheng and G. Zhao, Enantioselective Vinylogous Mannich-Type Reactions to Construct CF₃S-Containing Stereocenters Catalysed by Chiral Quaternary Phosphonium Salts, *Adv. Synth. Catal.*, 2020, **362**(9), 1851–1857.

31 H. Hong, C. Zheng, G. Zhao and Y. Shang, Enantioselective Michael Addition Reactions to Construct SCF₃-containing Stereocenter Catalyzed by Chiral Quaternary Phosphonium Salts, *Adv. Synth. Catal.*, 2020, **362**(24), 5765–5771.

32 M. Deliaval, R. Jayarajan, L. Eriksson and K. J. Szabó, Three-Component Approach to Densely Functionalized Trifluoromethyl Allenols by Asymmetric Organocatalysis, *J. Am. Chem. Soc.*, 2023, **145**(18), 10001–10006.

33 R. Jayarajan, T. Kireilis, L. Eriksson and K. J. Szabó, Asymmetric Organocatalytic Homologation: Access to Diverse Chiral Trifluoromethyl Organoboron Species, *Chem. – Eur. J.*, 2022, **28**(58), e202202059.

34 K. J. Szabó, Fluorination, Trifluoromethylation, and Trifluoromethylthiolation of Alkenes, Cyclopropanes, and Diazo Compounds, in *Organofluorine Chemistry*, 2021, pp. 201–223.

35 S. J. T. Jonker, R. Jayarajan, T. Kireilis, M. Deliaval, L. Eriksson and K. J. Szabó, Organocatalytic Synthesis of α-Trifluoromethyl Allylboronic Acids by Enantioselective 1,2-Borotropic Migration, *J. Am. Chem. Soc.*, 2020, **142**(51), 21254–21259.

36 F. Shen, P. P. Zhang, L. Lu and Q. Shen, [[(Ethoxycarbonyl) difluoromethyl]thio]phthalimide: A Shelf-Stable, Electrophilic Reagent with a Convertible Group for the Synthesis of Diversified Fluoroalkylthiolated Compounds, *Org. Lett.*, 2017, **19**(5), 1032–1035.

37 Q. Wang, T. Nilsson, L. Eriksson and K. J. Szabó, Sulfenofunctionalization of Chiral α-Trifluoromethyl Allylboronic Acids: Asymmetric Synthesis of SCF₃, SCF₂R, SCN and SAr Compounds, *Angew. Chem., Int. Ed.*, 2022, **61**(46), e202210509.

38 A. Matviitsuk, J. L. Panger and S. E. Denmark, Catalytic, Enantioselective Sulfenofunctionalization of Alkenes: Development and Recent Advances, *Angew. Chem., Int. Ed.*, 2020, **59**(45), 19796–19819.

39 H.-Y. Luo, Z.-H. Li, D. Zhu, Q. Yang, R.-F. Cao, T.-M. Ding and Z.-M. Chen, Chiral Selenide/Achiral Sulfonic Acid Cocatalyzed Atroposelective Sulfenylation of Biaryl Phenols via a Desymmetrization/Kinetic Resolution Sequence, *J. Am. Chem. Soc.*, 2022, **144**(7), 2943–2952.

40 A. D. Becke, Density-unctional Exchange-energy Approximation with Correct Asymptotic Behavior, *Phys. Rev. A*, 1988, **38**(6), 3098–3100.

41 A. D. Becke, Density–functional Thermochemistry. III. The Role of Exact Exchange, *J. Chem. Phys.*, 1993, **98**(7), 5648–5652.

42 S. Grimme, J. Antony, S. Ehrlich and H. Krieg, A Consistent and Accurate ab initio Parametrization of Density Functional Dispersion Correction (DFT-D) for the 94 Elements H-Pu, *J. Chem. Phys.*, 2010, **132**(15), 154104.

43 S. Grimme, S. Ehrlich and L. Goerigk, Effect of the Damping Function in Dispersion Corrected Density Functional Theory, *J. Comput. Chem.*, 2011, **32**(7), 1456–1465.

44 M. J. Frisch, G. W. Trucks, H. B. Schlegel, G. E. Scuseria, M. A. Robb, J. R. Cheeseman, G. Scalmani, V. Barone, G. A. Petersson, H. Nakatsuji, X. Li, M. Caricato, A. V. Marenich, J. Bloino, B. G. Janesko, R. Gomperts, B. Mennucci, H. P. Hratchian, J. V. Ortiz, A. F. Izmaylov, J. L. Sonnenberg, D. Williams-Young, F. Ding, F. Lipparini, F. Egidi, J. Goings, B. Peng, A. Petrone, T. Henderson, D. Ranasinghe, V. G. Zakrzewski, J. Gao, N. Rega, G. Zheng, W. Liang, M. Hada, M. Ehara, K. Toyota, R. Fukuda, J. Hasegawa, M. Ishida, T. Nakajima, Y. Honda, O. Kitao, H. Nakai, T. Vreven, K. Throssell, J. A. Montgomery Jr., J. E. Peralta, F. Ogliaro, M. J. Bearpark, J. J. Heyd, E. N. Brothers, K. N. Kudin, V. N. Staroverov, T. A. Keith, R. Kobayashi, J. Normand, K. Raghavachari, A. P. Rendell, J. C. Burant, S. S. Iyengar, J. Tomasi, M. Cossi, J. M. Millam, M. Klene, C. Adamo, R. Cammi, J. W. Ochterski, R. L. Martin, K. Morokuma, O. Farkas, J. B. Foresman and D. J. Fox, *Gaussian 16 Rev. C.01*, Wallingford, CT, 2016.

45 A. V. Marenich, C. J. Cramer and D. G. Truhlar, Universal Solvation Model Based on Solute Electron Density and on a Continuum Model of the Solvent Defined by the Bulk Dielectric Constant and Atomic Surface Tensions, *J. Phys. Chem. B*, 2009, **113**(18), 6378–6396.

46 S. E. Denmark, E. Hartmann, D. J. P. Kornfilt and H. Wang, Mechanistic, Crystallographic, and Computational Studies on the Catalytic, Enantioselective Sulfenofunctionalization of Alkenes, *Nat. Chem.*, 2014, **6**(12), 1056–1064.

47 X.-F. Song, T.-M. Ding, D. Zhu, J. Huang and Z.-M. Chen, Lewis-Acid-Mediated Intramolecular Trifluoromethylthiolation of Alkenes with Phenols: Access to SCF₃-Containing Chromane and Dihydrobenzofuran Compounds, *Org. Lett.*, 2020, **22**(17), 7052–7056.

48 Q. Jiang, H. Li and X. Zhao, Catalytic Electrophilic Thiocarbocyclization of Allenes, *Org. Lett.*, 2021, **23**(22), 8777–8782.

This journal is © the Partner Organisations 2025

Org. Chem. Front., 2025, **12**, 2994–3003 | **3003**